Low-loss ultra-high-Q dark mode plasmonic Fano metamaterials

Wei Cao,[1] Ranjan Singh,[2,5,*] Ibraheem A. I Al-Naib,[3] Mingxia He,[4] Antoinette J. Taylor,[2] and Weili Zhang[1,6]

[1]*School of Electrical and Computer Engineering, Oklahoma State University, Stillwater, Oklahoma 74078, USA*

[2]*Center for Integrated Nanotechnologies, Materials Physics and Applications Division, Los Alamos National Laboratory, Los Alamos, New Mexico 87545, USA*

[3]*INRS-EMT, 1650 Boul. Lionel-Boulet, Varennes, Québec J3X 1S2, Canada*

[4]*Center for Terahertz Waves and College of Precision Instrument and Optoelectronics Engineering, Tianjin University, Tianjin 300072, China*

[5]*email: ranjan@lanl.gov*

[6]*email: weili.zhang@okstate.edu*

**Corresponding author: ranjan.ranjansingh@gmail.com*

Received April 6, 2012; revised June 11, 2012; accepted July 10, 2012;
posted July 10, 2012 (Doc. ID 166248); published August 7, 2012

We experimentally demonstrate a planar terahertz Fano metamaterial with an ultrahigh quality (Q) factor of 227. This is achieved by the excitation of the nonradiative dark modes by introducing a tiny asymmetry in the metamaterial structure. The extremely sharp quadrupole and Fano resonances are excited at normal incidence for orthogonal polarizations of the electric field. In order to capture the narrow linewidth of the dark resonance modes, we perform high resolution terahertz time–domain measurements with a scan length of 200 picoseconds and frequency resolution of 5 GHz. These high-Q metamaterials can be used in ultrasensitive label-free terahertz sensing, dense photonic integration, and narrowband filtering.

OCIS codes: 300.6495, 160.3918.

The most fascinating aspect of the artificially designed plasmonic metamaterials is that they could easily be tailored for many different applications due to their exotic response to the electromagnetic waves. However, substantial losses in conventional metamaterials have restricted the development of efficient devices in the terahertz, infrared, and optical frequency regimes. The loss in metamaterials arises from the Ohmic resistance of the materials used to fabricate the metamolecules and the radiation resistance that is usually high in the planar plasmonic resonators. Metals are the most widely used materials for fabricating metamolecules such as split-ring resonators, due to their high conductivity. At optical and near-infrared frequencies, even the highest conducting metals exhibit Ohmic losses, thus requiring the discovery of a new plasmonic material [1,2]. Fortunately, at far infrared terahertz frequencies, the most commonly used metals (Ag, Al, and Au) for plasmonic metamaterials have much higher conductivity and they almost behave as perfect conductors. This perfect conduction ensures much lower resistive losses [3,4].

Despite lower Ohmic losses at terahertz frequencies, there has been no significant improvement in the quality factor (Q) of the metamaterial resonances due to the existing radiative losses. Typically, the Q-factor in the terahertz, infrared, and optical plasmonic metamaterials is less than 10 [1–4].

In this Letter, we report an extremely high Q-factor of 227 in planar terahertz metamaterial by suppressing the radiative losses tremendously through the excitation of dark quadrupole and Fano resonances. This Q-factor value is at least four times higher than all previous demonstrations [3–16]. The asymmetric split ring (ASR) is excited at normal incidence and a high-Q bandpass resonance is observed for the x-polarized electric field excitation (Fig. 1). Such high Q-factors will allow the metamaterials to be used in several device applications, particularly for ultrasensitive label-free sensors [17–20]. Apart from sensing applications, the subwavelength high-Q metamaterial cavities can be applied to improve the performance of switches, memories, modulators, and single photon emitters.

We employ photoconductive switch based broadband terahertz (THz) time-domain spectroscopy to characterize the metamaterials. Seven sets of ASR metamaterial samples were fabricated on high-resistivity ($4\ \mathrm{k}\Omega\cdot\mathrm{cm}$), double-side polished, 0.5 mm thick n-type silicon substrate using conventional photolithography, and then a 200 nm thick aluminum was thermally metallized to form the ASRs. A 10 mm thick, high-resistivity ($4\ \mathrm{k}\Omega\cdot\mathrm{cm}$) silicon plate was placed in optical contact with the backside of the metamaterial substrate to eliminate the reflection from the substrate bottom surface and allow us to scan up to 200 ps, thus enabling a frequency resolution of 5 GHz.

Asymmetry in the ASRs is introduced by displacing the lower gap gradually from the central vertical axis, as shown in the inset of Fig. 1(b), with $d = 1$, 2, 3, 4, 5, 10, and 20 μm, respectively, where d represents the lower gap displacement from the center. We would address them as ASR1 ($d = 1\ \mu$m), ASR2 ($d = 2\ \mu$m), ASR3 ($d = 3\ \mu$m), ASR4 ($d = 4\ \mu$m), ASR5 ($d = 5\ \mu$m), ASR10 ($d = 10\ \mu$m), and ASR20 ($d = 20\ \mu$m). The sample array size is 10 mm $\times$ 10 mm, and $\sim$1710 ASRs are excited by the collimated terahertz beam of 3.5 mm in diameter.

The time-domain data were taken for all seven metamaterial samples in a sequential order for two orthogonal orientations of the electric terahertz field. Figure 1(a) shows the measured long scan (200 ps) terahertz pulses transmitted through ASR5 and the reference blank silicon to be identical to the metamaterial substrate, both

0146-9592/12/163366-03$15.00/0

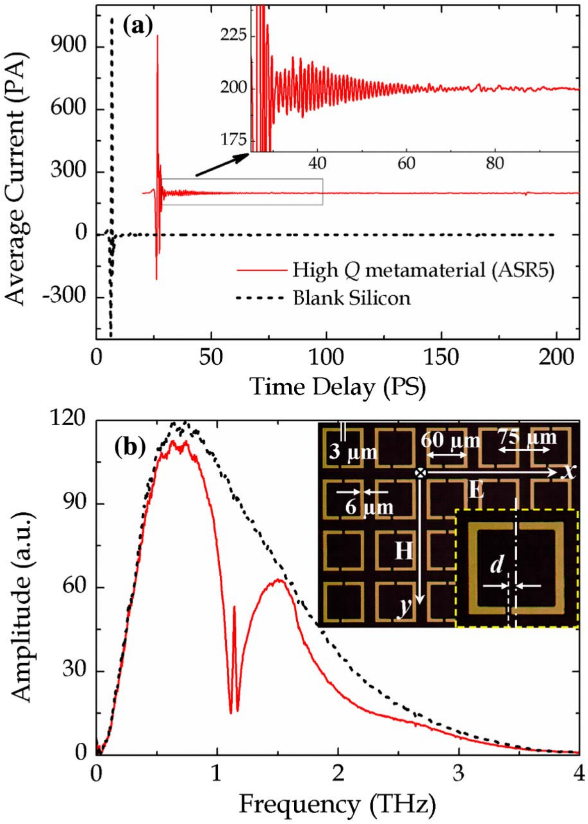

Fig. 1. (Color online) (a) Measured time-domain transmission through metamaterial ASR5 and the blank silicon. Inset: strong time-domain ringing beyond the main terahertz pulse. (b) Corresponding Fourier transform of the measured pulses. Inset: Image of ASR5.

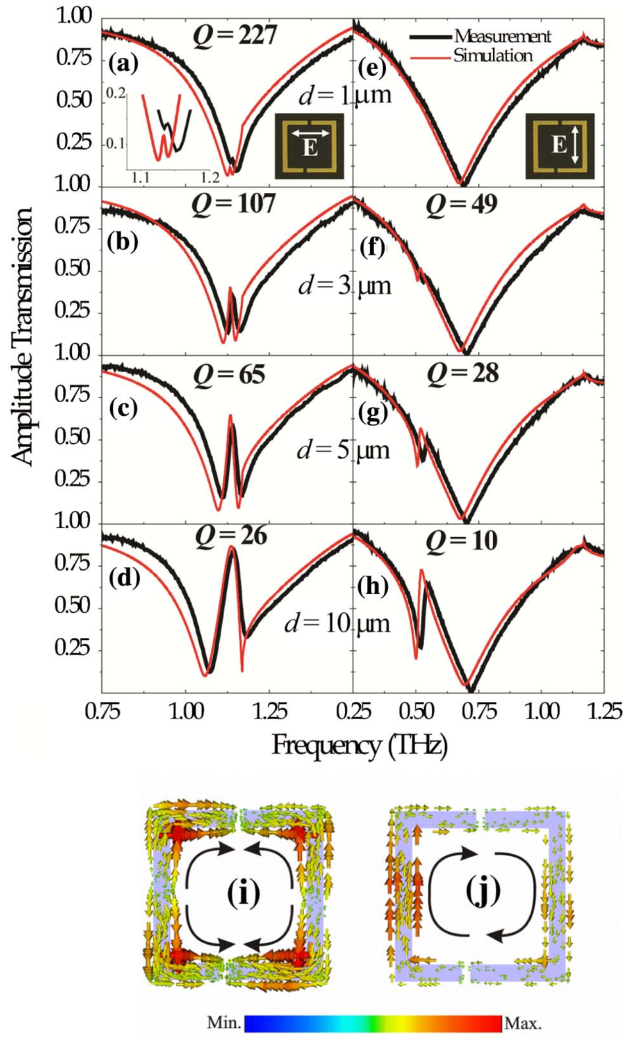

Fig. 2. (Color online) Measured and simulated transmission spectra when (a)–(d) the E field is polarized along the gaps arms, and (e)–(h) the E field is polarized perpendicular to the gap arms in ASR1, ASR3, ASR5, and ASR10, respectively. The inset graphs in (a) illustrate the zoomed resonance feature of ASR1. Surface current simulations in ASR5 at (i) transmission resonance peak at 1.14 THz when the E field is along the gap in the x direction, (j) transmission resonance dip at 0.5 THz when the E field is perpendicular to the gap in the y direction.

attached with the 10 mm thick silicon while the E field is along the ASR5 gap arms in the x direction. A strong oscillation in the pulse is observed at a later time, as shown in the inset of Fig. 1(a). The Fourier transform of the time-domain pulses is shown in Fig. 1(b), which clearly reveals a very sharp bandpass resonance feature with a high-Q-factor. All the spectra were calculated by zero padding, i.e., 200 ps data pulse was extended to 400 ps by adding zeros at the end of the pulse. This is done to interpolate between measured data points that are separated here by 5 GHz. The frequency resolution in all the simulations using CST Microwave Studio is 0.38 GHz.

Figures 2(a)–2(d) show the measured and simulated transmission spectra through samples of ASR1, ASR3, ASR5, and ASR10 with increasing degree of structural asymmetry when the incident E field is linearly polarized along the gap containing arms in the x direction. An ultrasharp transparency peak gradually evolves at 1.14 THz as the structural asymmetry is increased.

It should be noted that this particular resonance is forbidden in a perfect symmetry structure ($d = 0$); thus, it is a dark mode that has a quadrupolar nature as will be discussed later by looking at the simulated surface currents. In the case of perfect symmetrical structure, only a bright dipolar resonance that is highly radiative in nature is excited since the currents in the two equal metal wire arms oscillate in phase and interfere constructively. In the ASRs, as one of the gaps is moved away from the vertical axis, the resonance frequencies of the two metallic wires forming the ASR differ by a small value, leading to a strong coupling between them. This results in an out-of-phase oscillation for an extremely narrow range of frequencies, causing a destructive interference that opens up a high-Q transparency sub-band in the background spectrum of a broad dipole resonance. The best Q-factor of 227 is observed for the lowest asymmetry case in ASR1, though the resonance feature is extremely weak. Beyond that, as the bottom gap is moved away from the center, the Q decreases but the transmission gets enhanced. In order to quantize the tradeoff between the Q-factor and the resonant transmission, we define the product of Q and resonance amplitude (A) as the figure of merit (FOM) $= Q * A$. The FOM of all the structures is plotted in the inset of Fig. 3(a) and we obtain the best FOM $= 47$ for ASR4 with a Q of 83.5 and transmission of 56%.

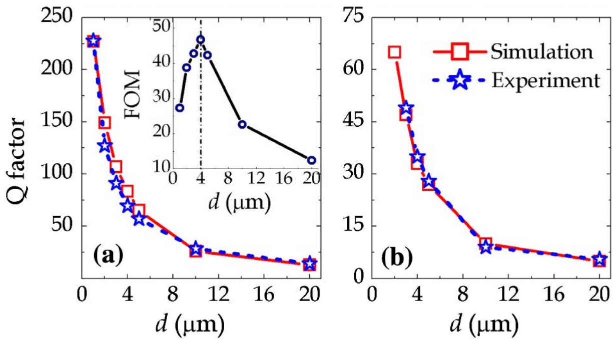

Fig. 3. (Color online) Q-factors calculated from the measurement and simulations for (a) E field along the gap and (b) E field perpendicular to the gap. The inset of (a) shows the figure of merit.

Figures 2(e)–2(h) show the transmission response of ASRs when the E field is along the vertical axis in the y direction. At this orientation, the high Q band stop resonance mode excited at 0.5 THz is the asymmetric Fano resonance that is also dark in nature, and can be excited only when the symmetry of the structure is broken [12–16,21]. Figure 2(i) shows the simulated surface currents at the transparency resonant peak (1.14 THz) for structure ASR5, and it reveals a quadrupole current distribution. This mode is excited only when the system symmetry is broken, leading to a destructive interference between the bright dipolar mode and the dark quadrupole mode. A broad dipolar resonance exists for the perfectly symmetric structure, and it is strongly coupled to the incident terahertz electromagnetic field, whereas the quadrupole mode couples weakly to the incident field. The existence of such narrow resonances implies extremely low losses, which in turn requires a significant reduction of radiative losses. Figure 2(j) shows the antiparallel surface current distribution of a typical subradiant Fano resonance when ASR5 is excited with incident E field in the y direction.

In Figs. 3(a) and 3(b), we have plotted the experimental and the simulated Q at the quadrupole resonance transparency and the Fano resonance, respectively, as a function of asymmetry parameter. The Q is calculated from the power transmission spectra, and since the resonance feature has an asymmetric line shape, we chose the highest peak and the lowest dip on the resonance curve as two extreme points and then noted the full width at half maximum (FWHM $= \Delta f$) bandwidth. Taking the ratio of the resonance frequency, f_0 and the FWHM, i.e. $(f_0/\Delta f)$, we obtained the value of Q. It is interesting to observe that the Q-factors of quadrupole and Fano resonances have a very similar declining pattern that resembles an exponential decay with the increase in the degree of asymmetry. This happens due to the exponential decay of the near fields in the two excited wire arms as the coupling strength between them reduces with increase in asymmetry.

In conclusion, we have successfully demonstrated ultrahigh-Q resonances at normal incidence for x- and y-polarizations of the incident electric field. As soon as the symmetry of the split ring structure was reduced, we observe the evolution of the quadrupole and the Fano resonances for two different excitations. This finding will pave the path for design of ultrahigh-Q low loss plasmonic metamaterials for multifunctional applications such as ultrasensitive terahertz and optical label free sensors and narrowband terahertz and optical filters.

This work was partially supported by the U.S. National Science Foundation and the National Science Foundation of China (Grants No. 61138001 and No. 61028011). R. S. acknowledges support from Center of Integrated Nanotechnologies, a United States Department of Energy (DOE), Office of Basic Energy Sciences Nanoscale Science Research Center operated jointly by Los Alamos and Sandia National Laboratories.

References

1. A. Boltasseva and H. A. Atwater, Science **331**, 290 (2011).
2. J. B. Khurgin and G. Sun, Appl. Phys. Lett. **99**, 211106 (2011).
3. R. Singh, A. K. Azad, J. F. O'Hara, A. J. Taylor, and W. Zhang, Opt. Lett. **33**, 1506 (2008).
4. R. Singh, Z. Tian, J. Han, C. Rockstuhl, J. Gu, and W. Zhang, Appl. Phys. Lett. **96**, 071114 (2010).
5. N. Liu, L. Langguth, T. Weiss, J. Kästel, M. Fleischhauer, T. Pfau, and H. Giessen, Nat. Mater. **8**, 758 (2009).
6. C. Jansen, I. A. I. Al-Naib, N. Born, and M. Koch, Appl. Phys. Lett. **98**, 051109 (2011).
7. A. Bitzer, J. Wallauer, H. Helm, H. Merbold, T. Feurer, and M. Walther, Opt. Express **17**, 22108 (2009).
8. R. Singh, C. Rockstuhl, and W. Zhang, Appl. Phys. Lett. **97**, 241108 (2010).
9. R. Singh, I. A. I. Al-Naib, M. Koch, and W. Zhang, Opt. Express **19**, 6312 (2011).
10. C. Ropers, D. J. Park, G. Stibenz, G. Steinmeyer, J. Kim, D. S. Kim, and C. Lienau, Phys. Rev. Lett. **94**, 113901 (2005).
11. I. A. I. Al-Naib, C. Jansen, N. Born, and M. Koch, Appl. Phys. Lett. **98**, 091107 (2011).
12. V. A. Fedotov, M. Rose, S. L. Prosvirnin, N. Papasimakis, and N. I. Zheludev, Phys. Rev. Lett. **99**, 147401 (2007).
13. R. Singh, I. A. I. Al-Naib, Y. P. Yang, D. R. Chowdhury, W. Cao, C. Rockstuhl, T. Ozaki, R. Morandotti, and W. L. Zhang, Appl. Phys. Lett. **99**, 201107 (2011).
14. A. E. Miroshnichenko, S. Flach, and Y. S. Kivshar, Rev. Mod. Phys. **82**, 2257 (2010).
15. R. Singh, I. A. I. Al-Naib, M. Koch, and W. Zhang, Opt. Express **18**, 13044 (2010).
16. B. Luk'yanchuk, N. I. Zheludev, S. A. Maier, N. J. Halas, P. Nordlander, H. Giessen, and C. T. Chong, Nat. Mater. **9**, 707 (2010).
17. C. Wu, A. B. Khanikaev, R. Adato, N. Arju, A. A. Yanik, H. Altug, and G. Shvets, Nat. Mater. **11**, 69 (2011).
18. J. F. O'Hara, R. Singh, I. Brener, E. Smirnova, J. Han, A. J. Taylor, and W. Zhang, Opt. Express **16**, 1786 (2008).
19. J. Zhao, C. Zhang, P. V. Braun, and H. Giessen, Adv. Mater. (to be published).
20. J. F. O'Hara, W. Withayachumnankul, and I. A. I. Al-Naib, Terahertz **33**, 245 (2012).
21. U. Fano, Phys. Rev. **124**, 1866 (1961).